



Structural evolution and second harmonic properties of lithium niobate–tantalate nanocrystals embedded in a borate glass



P.W. Jaschin, K.B.R. Varma *

Materials Research Centre, Indian Institute of Science, Bangalore 560012, India

ARTICLE INFO

Article history:

Received 10 October 2015

Received in revised form 2 December 2015

Accepted 19 December 2015

Available online xxxx

Keywords:

Glass nanocrystal composites

Lithium niobate

Lithium tantalate

Second harmonic generation

Coalescence

ABSTRACT

Nano-crystals of $\text{LiNb}_x\text{Ta}_{1-x}\text{O}_3$ were evolved by subjecting melt-quenched $1.5\text{Li}_2\text{O}-2\text{B}_2\text{O}_3-x\text{Nb}_2\text{O}_5-(1-x)\text{Ta}_2\text{O}_5$ glasses (where $x = 0, 0.25, 0.5, 0.75$ and 1.00) to a controlled 3-h isothermal heat treatment between 530 and 560 °C. Detailed X-ray diffraction and Raman spectral studies confirmed the formation of nano-crystalline $\text{LiNb}_x\text{Ta}_{1-x}\text{O}_3$ along with a minor phase of ferroelectric and non-linear optic $\text{Li}_2\text{B}_4\text{O}_7$. The sizes of the nanocrystals evolved in the glass were in the range of 19–37 nm for $x = 0-0.75$ and 23–45 nm for $x = 1.00$. Electron microscopic studies confirmed a transformation of the morphology of the nano-crystallites from dendritic star-shaped spherulites for $x = 0$ to rod-shaped structures for $x = 1.00$ brought about by a coalescence of crystallites. Broad Maker-fringe patterns (recorded at 532 nm) were obtained by subjecting the heat-treated glass plates to 1064 nm fundamental radiation. However, an effective second order non-linear optic coefficient, d_{eff} , of 0.45 pm/V, which is nearly 1.2 times the d_{36} of KDP single crystal, was obtained for a 560 °C/3 h heat-treated glass of the representative composition $x = 0.50$ comprising 37 nm sized crystallites.

© 2015 Elsevier B.V. All rights reserved.

1. Introduction

A glass/polymer-based nano-crystal composite route provides an economically viable and less time-consuming method for generating multi-functional materials that can substitute single crystals in several device applications [1–6]. However, glass nanocrystal composites are preferred as they have relatively high mechanical strength, thermal stability and laser damage threshold. Several ferroelectric oxides including BaTiO_3 [7], $\text{Sr}_{0.5}\text{Ba}_{0.5}\text{Nb}_2\text{O}_6$ [8], $\text{Ba}_2\text{NaNb}_5\text{O}_{15}$ [9], and $\text{Bi}_2\text{VO}_{5.5}$ [10], have been crystallized in glass matrices. Applications of glass–ceramics and glass nanocrystal composites are not just limited to their optical properties as their electrical properties are also being exploited in devices such as high energy density capacitors [11], pyroelectrics [12], and piezoelectrics [13]. Facile and low cost fabrication, control over microstructure, tunability of physical properties, low thermal expansion and good thermal stability are a few of the many advantages that glass–ceramics provide for device applications. Melt-quenching, roller-quenching and sol-gel techniques are conventionally employed to fabricate amorphous materials, which are further heat-treated under isothermal conditions to induce nano/micro-crystallization in the system.

Lithium tantalate, LiTaO_3 , and lithium niobate, LiNbO_3 , are two of the best available perovskite oxides for electro-optic, non-linear optic and acousto-optic device applications. LiTaO_3 and LiNbO_3 are isostructural crystals belonging to the space group $R3c$, with lattice parameters $a =$

5.15428 \AA , $c = 13.7835 \text{ \AA}$ and $a = 5.14739 \text{ \AA}$, $c = 13.85614 \text{ \AA}$, respectively [14,15]. LiTaO_3 and LiNbO_3 are ferroelectric and piezoelectric at room temperature and undergo ferroelectric-to-paraelectric transition at 620 °C and 1210 °C, respectively [16]. The remnant polarization is as high as $55 \mu\text{C}/\text{cm}^2$ for LiTaO_3 and $75 \mu\text{C}/\text{cm}^2$ for LiNbO_3 [17]. LiTaO_3 and LiNbO_3 also exhibit promising non-linear optical properties associated with reasonably high non-linear optical coefficients [18]. Tunability of several physical properties can, hence, be achieved with solid solutions of LiTaO_3 and LiNbO_3 . For example, tailored compositions of $\text{LiNb}_x\text{Ta}_{1-x}\text{O}_3$ single crystals have shown tremendous enhancement in performance and speed when used as a polarization mode dispersion compensator for signal transmission across optical fibers [19]. Composition-dependent properties such as refractive index, dielectric [18] optical birefringence [20] and waveguiding [21] have been reported in the literature. Theoretical studies on the solid solutions show that the non-linear susceptibility is linearly dependent on Ta/Nb ratio, the d -coefficient increasing linearly with the Nb content [18]. Glasses with $\text{LiNb}_{0.5}\text{Ta}_{0.5}\text{O}_3$ nanocrystals have previously been fabricated only by the sol-gel route. Moreover, their physical properties have so far not been discussed widely [22].

In our recent article on the pyroelectric properties of LiTaO_3 glass–ceramics, a brief discussion on the second harmonic properties (optical) associated with its crystallite size was elucidated [23]. In this report, we report on embedding $\text{LiNb}_x\text{Ta}_{1-x}\text{O}_3$ nanocrystals in a borate-based glass matrix and variation in microstructure and optical second harmonic properties as a function of Nb/Ta ratio. The glass composition was chosen in such a way that the inevitable minor impurity phase

* Corresponding author.

E-mail address: kbrvarma@mrcc.iisc.ernet.in (K.B.R. Varma).

that crystallizes along with the major $\text{LiNb}_x\text{Ta}_{1-x}\text{O}_3$ phase was $\text{Li}_2\text{B}_4\text{O}_7$, which is also a ferroelectric and an active non-linear optic material.

2. Experimental

Isothermal heat treatment of glasses in the $1.5\text{Li}_2\text{O}-2\text{B}_2\text{O}_3-x\text{Nb}_2\text{O}_5-(1-x)\text{Ta}_2\text{O}_5$ system, where in $x = 0, 0.25, 0.5, 0.75$ and 1.00 , at appropriate temperatures yielded the desired $\text{LiNb}_x\text{Ta}_{1-x}\text{O}_3$ phase along with the minor crystalline $\text{Li}_2\text{B}_4\text{O}_7$ impurity phase. To obtain the glasses (by melt-quenching technique), Li_2CO_3 (S.D. Fine Chemical, 99%), Ta_2O_5 (Aldrich, 99.99%), Nb_2O_5 (Aldrich, 99.99%) and H_3BO_3 (Emparta ACS, 99.5%) were chosen in stoichiometric amounts and melted in a platinum crucible in $1200-1300^\circ\text{C}$ temperature range for about 30 min in a Lenton electric furnace. The batch weight was 8 g. The melt was then quickly poured on a steel plate maintained at 150°C and pressed by another plate. Optically transparent plates of 1 mm thickness and 10 cm diameter were obtained. In order to minimize any thermal stress likely to be induced by the quenching process, the as-quenched samples were annealed at 250°C for 5 h (which is well below their glass transition temperatures). Prior to the heat treatment, rectangularly cut samples were subjected to optical quality polishing. The samples were heated at $530, 540, 550$ and 560°C for 3 h at a heating rate of $3^\circ\text{C}/\text{min}$, and subsequently furnace-cooled.

Thermal analysis of the as-quenched glasses was performed by a differential scanning calorimeter (Perkin Elmer Diamond DSC) between 50 and 650°C at a heating rate of $10^\circ\text{C}/\text{min}$. The densities of the samples were measured to an accuracy of $\pm 0.01 \text{ g}/\text{cm}^3$ using Archimedes' principle, with xylene as a buoyancy medium. XRD patterns were recorded by a PanAnalytical X-pert Pro X-ray diffractometer at room temperature using $\text{Cu-K}\alpha$ radiation operating at $40 \text{ kV}/30 \text{ mA}$. Rietveld refinement of the XRD data was done using the General Structure Analysis System (GSAS) [24,25]. The background was corrected with shifted Chebyshev function and pseudo-Voigt function was employed to model the observed Bragg reflections. The volume fraction of crystallization of the $\text{LiNb}_x\text{Ta}_{1-x}\text{O}_3$ phase in the heat-treated samples was obtained from XRD peak intensities with KCl as the standard (1:1 weight ratio) as there was no overlap of the strongest diffraction peaks of these two compounds. Raman spectra were recorded for the $560^\circ\text{C}/3 \text{ h}$ heat-treated samples between 50 and 1200 cm^{-1} by using a WiTec Alpha 300 Raman spectrometer in 180° back-scattering geometry. A frequency-doubled Nd-YAG (532 nm) laser was used as the excitation source. The spectral resolution was 3 cm^{-1} .

An FEI Inspect F50 scanning electron microscope and a JEOL 2100F transmission electron microscope were employed for microstructural analysis of the heat-treated samples. A double-beam UV-vis spectrophotometer (Perkin-Elmer Lambda 750 UV/vis/NIR spectrophotometer) with a $200-2500 \text{ nm}$ spectral range was used to record the transmission spectra of the as-quenched samples. Refractive indices of the as-quenched glasses were determined at $\lambda = 532 \text{ nm}$ using Brewster angle technique. A fundamental wave of pulsed Nd-YAG laser operating at 1064 nm (Q-switched mode), producing 10 ns pulses at 10 Hz , was used for the optical second harmonic studies. Second harmonic signals (at 532 nm) emanating from the heat-treated samples were recorded using a monochromator in conjunction with a photomultiplier tube.

3. Results and discussion

The thermal properties of the as-quenched samples were studied by DSC. Fig. 1 depicts the DSC traces obtained for the as-quenched samples. Typical endotherms and exotherms are encountered in all the curves, which correspond to glass transition (T_g) and crystallization temperatures (T_{cr}), respectively. The values of the T_g are in the range of $470-490^\circ\text{C}$, depending on the x value. The two sharp exothermic peaks in the $560-580^\circ\text{C}$ range observed for $x = 0$ are attributed to the crystallization of LiTaO_3 and $\text{Li}_2\text{B}_4\text{O}_7$ phases [23]. However, with

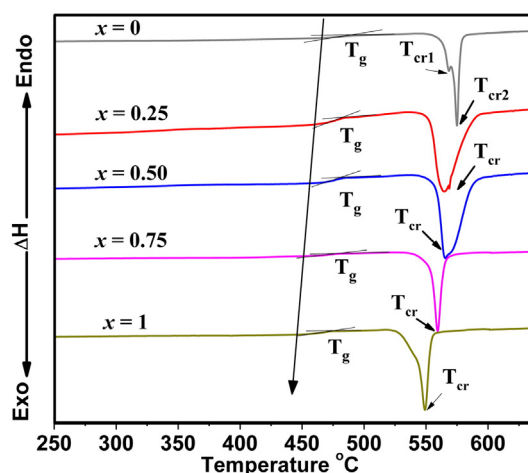


Fig. 1. DSC curves of the as-quenched glasses of all compositions under study.

increasing x values, only one broad crystallization peak appears. The peaks are particularly broad at $x = 0.25$ and 0.50 , which is ascribed to either crystallization of two or more phases or surface crystallization. XRD analysis, to be discussed below, shows an additional phase of $\text{Li}_2\text{B}_4\text{O}_7$ crystallizing in the glasses of all the compositions. The additional phase influences the broadness associated with the exothermic peaks. For $x = 0.75$ and 1.00 , the exotherms appear to have shoulders, suggesting the presence of two closely-crystallizing phases. The values of T_{cr} and T_g decrease with increasing x , probably due to the formation of more non-bridging oxygens upon raising the niobium content in the glass network. This may be justified based on the higher bond energy for Ta-O ($804.2 \text{ kJ}/\text{mol}$) than for Nb-O ($752 \text{ kJ}/\text{mol}$) [26]. The thermal parameters for the as-quenched glasses of all the compositions obtained from the DSC studies are presented in Table 1. The onset of crystallization temperature is identified as the temperature corresponding to the intersection of the two linear portions from the elbow of the exothermic peak. The onsets of crystallization appear to decrease on addition of Nb, from 556°C for the composition corresponding to $x = 0$ to 528°C for $x = 1$. The thermal stability of the glasses was also evaluated from the DSC curves. The thermal stability (ΔT), in a gross sense, is defined by the difference between the crystallization temperature and the glass transition temperature, ($T_{cr} - T_g$), which is the ability of a glass to resist crystallization. The thermal stability for the as-quenched glass corresponding to the composition $x = 0$ was determined from the difference between the first crystallization peak, T_{cr1} , and the glass transition temperature, T_g . The thermal stability is relatively high for the intermediate compositions ($x = 0.25, 0.50$ and 0.75) as compared to that for $x = 0$ and 1.00 (Table 1). The as-quenched glasses were subsequently heat-treated at $530, 540, 550$ and 560°C for 3 h to induce nanocrystallization of the desired phase. Optically transparent glasses systematically turned more translucent when subjected to heat treatment. The bulk crystallization of glass ceramics was observed under heat-treatment as the XRD pattern (not shown here) obtained even after polishing to a few micrometers depth showed the polycrystalline nature of the glass-nanocrystal composites.

Table 1
Thermal properties of the as-quenched glasses derived from DSC plots.

Composition x	0	0.25	0.50	0.75	1.00
T_g	489°C	483°C	481°C	478°C	473°C
T_{cr1}	567°C	565°C	563°C	559°C	548°C
T_{cr2}	574°C	–	–	–	–
Onset of crystallization	556°C	547°C	552°C	537°C	528°C
ΔT	77°C	82°C	82°C	81°C	75°C

Download English Version:

<https://daneshyari.com/en/article/7900842>

Download Persian Version:

<https://daneshyari.com/article/7900842>

[Daneshyari.com](https://daneshyari.com)